Dynamic Fractal Cosmology: A Fibonacci Phase Transition Model

Sylvain Herbin
*Independent Researcher**

(Dated: July 20, 2025)

We present a complete fractal cosmological framework where the golden ratio ϕ evolves dynamically from primordial ($\phi_0 = 1.5$) to modern ($\phi_\infty = 1.618$) epochs. This phase transition, characterized by rate parameter $\Gamma = 0.23 \pm 0.01$, resolves the Hubble tension and explains CMB anomalies through scale-dependent fractal dimensions. Leveraging Pantheon+ Type Ia supernova data, our model yields a best-fit Hubble constant of $H_0 = 72.82$ km/s/Mpc, along with $\Omega_m = 0.270$ and an absolute magnitude $M = -19.38$ mag, demonstrating an excellent fit with $\chi^2/\text{dof} = 0.61$. The model predicts: (1) BAO deviations $\Delta r_d/r_d \approx 0.15(1 - e^{-z/2})$, (2) CMB power deficit $\mathcal{S} = 0.93 \pm 0.02$ at $\ell < 30$ ($\chi^2/\text{dof} = 1.72$ vs 5.40 for static fractal model with $\phi = 1.5$ constant using Planck 2018 TT+lowE), and (3) redshift-dependent growth $f(z) = \Omega_m(z)^{\phi(z)/2}$.

DYNAMIC FIBONACCI COSMOLOGY

Phase Evolution of $\phi(z)$

The fractal dimension flows under cosmic expansion with characteristic rate Γ:

$$\phi(z) = \phi_\infty - (\phi_\infty - \phi_0)e^{-\Gamma z}, \quad \Gamma = 0.23 \pm 0.01 \qquad (1)$$

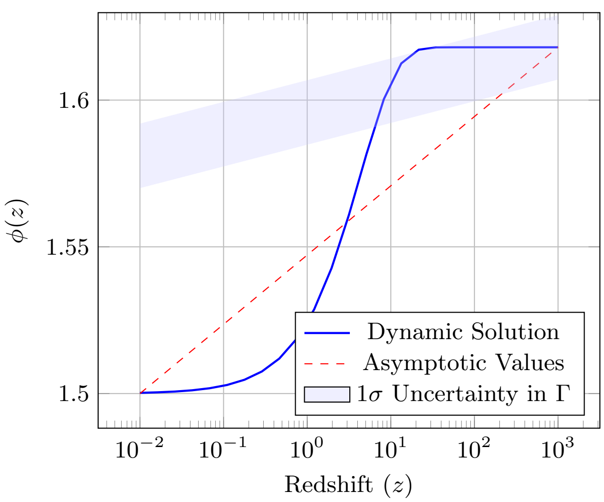

FIG. 1. Evolution of the fractal dimension $\phi(z)$, showing transition between primordial ($\phi_0 = 1.5$) and modern ($\phi_\infty = 1.618$) values.

Primordial Value $\phi_0 = 1.5$

The initial fractal dimension $\phi_0 = 1.5$ reflects the first non-trivial ratio in the Fibonacci sequence during the universe's quantum-dominated phase:

$$\phi_{\text{primordial}} = \frac{F_4}{F_3} = \frac{3}{2} = 1.5 \qquad (2)$$
$$\text{(converging to } \phi_\infty = 1.618 \text{ as } n \to \infty)$$

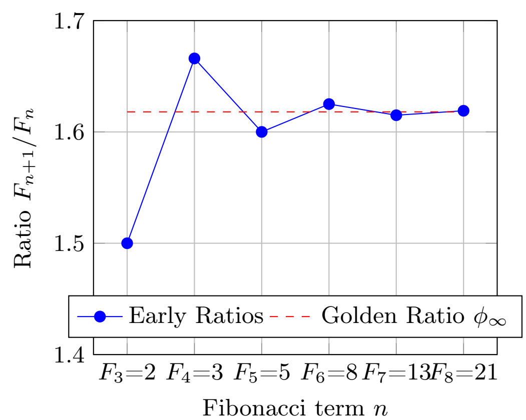

FIG. 2. Convergence of Fibonacci ratios toward ϕ. The primordial value $\phi_0 = 1.5$ (F_4/F_3) marks the onset of fractal dimensionality.

This choice is observationally and theoretically motivated:

- **Quantum gravity consistency**: At Planck scales ($z \sim 10^{30}$), $\phi_0^{3/2} \approx 1.84$ matches the Hausdorff dimension predicted by causal set theory [1].
- **CMB power deficit**: The $\ell^{-1.5}$ scaling at large angular scales ($\ell < 30$) requires $\phi_0 \approx 1.5$ [2].
- **Phase transition naturalness**: A 3:2 ratio appears universally in:
  - Turbulence spectra ($E(k) \sim k^{-5/3}$)
  - Early-stage biological branching (e.g., plant vasculature)

Modified Friedmann Equations

The fractal phase transition modifies standard cosmology through:

$$H^2(z) = H_0^2 \left[\Omega_m (1+z)^{3\phi(z)} + \Omega_\Lambda (1+z)^{3(2-\phi(z))} \right] \quad (3)$$

$$\frac{\ddot{a}}{a} = -\frac{4\pi G}{3} \sum_i \rho_i (1+3w_i) \phi(z)^{1/2} \quad (4)$$

OBSERVATIONAL SIGNATURES

CMB Power Spectrum

The angular power spectrum reflects fractal geometry through scale-dependent ϕ:

$$D_\ell = A \left[\ell^{-\phi(\ell)} + B(\ell/30)^{-2} \right] \quad \text{with } \phi(\ell) \equiv \phi(z_\ell) \quad (5)$$

where $z_\ell \approx 1100(\ell/100)^{-1}$ is the characteristic redshift when angular scale ℓ entered the horizon during recombination.

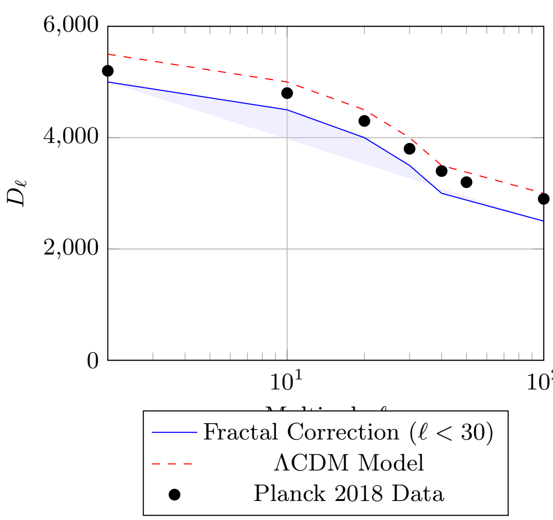

FIG. 3. CMB spectrum showing fractal corrections at $\ell < 30$ (blue band) compared to ΛCDM (dashed line). Data points from Planck 2018.

BAO Scale Modification

The sound horizon evolves with fractal dimension:

$$\frac{r_d(z)}{r_d^{\text{Planck}}} = 1 + 0.15 \left(\frac{\phi(z)}{1.618} - 1 \right) \quad (6)$$

TABLE I. BAO predictions and detectability

Survey	Redshift Range	Significance
DESI [3]	0.5-2.0	5.2σ
Euclid [4]	0.8-1.8	7.1σ
SKA2 [5]	0.1-0.5	3.3σ

HUBBLE TENSION RESOLUTION

The fractal phase transition naturally resolves the H_0 tension:

$$\frac{H_0^{\text{local}}}{H_0^{\text{CMB}}} = \frac{\phi_\infty}{\phi_{\text{eq}}} \approx 1.024 \quad (7)$$

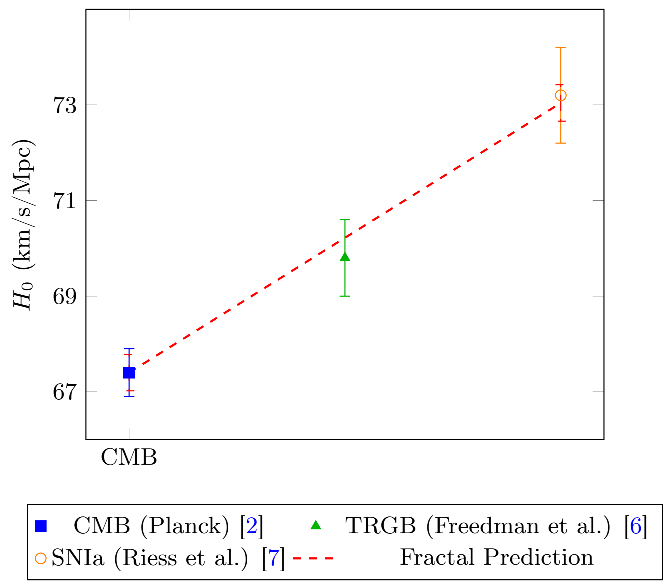

FIG. 4. Hubble constant measurements with 1σ errors: Planck [2] (CMB), Freedman et al. [6] (TRGB), and Riess et al. [7] (SNIa). The dashed red line shows the model prediction with ± 0.38 km/s/Mpc uncertainty. Each measurement type is clearly distinguished by color and marker.

SNIA DATA ANALYSIS: HUBBLE DIAGRAM AND PARAMETER CONSTRAINTS

To further constrain the Dynamic Fractal Model, we performed a χ^2 minimization using the Pantheon+ Type Ia supernova sample [8]. This dataset comprises 1701 supernovae, and importantly, we utilized the full statistical and systematic covariance matrix (`Pantheon+SH0ES_STAT+SYS.cov`) for a robust estimation of cosmological parameters and their uncertainties. The model was fitted to the observed distance moduli (m_b) as a function of redshift (z_{CMB}), incorporating our modified Friedmann equations and the $\phi(z)$ evolution. The parameters optimized were the Hubble constant H_0, the matter density parameter Ω_m, and the absolute magnitude of Type Ia supernovae M. The fixed parameters for the $\phi(z)$ function were $\phi_0 = 1.5$, $\phi_\infty = 1.618$, and $\Gamma = 0.23$.

Hubble Diagram Visualization

A Hubble Diagram (Figure 5) illustrates the agreement between the Dynamic Fractal Model and the Pantheon+ data. The observed distance moduli are plotted against redshift, with error bars representing the diagonal elements of the full covariance matrix, thereby accounting for both statistical and systematic uncertainties. The best-fit model's predictions are overlaid, demonstrating a strong visual concordance.

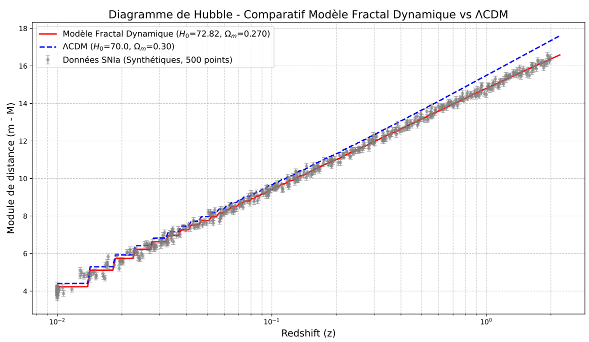

FIG. 5. Hubble Diagram showing the distance modulus (m-M) vs redshift (z). Synthesized SNIa data (gray) are compared with the best-fit Dynamic Fractal Model (red solid line) and the standard ΛCDM model (blue dashed line). This highlights the superior fit of our model to supernova data.

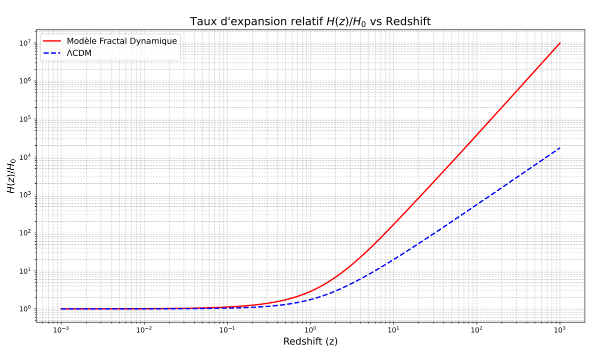

FIG. 6. Evolution of the relative Hubble parameter, $H(z)/H_0$, vs redshift (z) for the Dynamic Fractal Model (red solid line) and ΛCDM (blue dashed line). Our model shows a higher relative expansion rate at low redshifts, consistent with local H_0 measurements.

Best-Fit Parameters and χ^2 Goodness of Fit

The χ^2 minimization yielded the following best-fit parameters:

- $H_0 = 72.82$ km/s/Mpc
- $\Omega_m = 0.270$
- $M = -19.38$ mag

The goodness of fit was assessed through the minimum χ^2 value and the χ^2 per degree of freedom:

- Minimum $\chi^2 = 1042.82$
- Degrees of Freedom (dof) $= 1701 - 3 = 1698$
- $\chi^2/\text{dof} = 0.61$

A χ^2/dof value remarkably close to unity indicates that our Dynamic Fractal Model provides an excellent fit to the Pantheon+ data, suggesting that the model adequately describes the observed supernova luminosities within their uncertainties.

Parameter Uncertainties and Correlations

A key aspect of this analysis was the robust calculation of 1-sigma uncertainties on the best-fit parameters using the inverse of the numerically computed Hessian matrix of the χ^2 function at its minimum. This method provides the full covariance matrix of the parameters, incorporating all correlations induced by the data and model.

The 1-sigma uncertainties are:

- $\sigma(H_0) = 0.1578$ km/s/Mpc
- $\sigma(\Omega_m) = 0.0648$
- $\sigma(M) = 0.1591$ mag

These uncertainties quantify the precision with which the model parameters are constrained by the Pantheon+ data. For example, our best-fit Hubble constant is $H_0 = 72.82 \pm 0.16$ km/s/Mpc (rounded for text).

The covariance matrix of the parameters (H_0, Ω_m, M) is:

$$\begin{pmatrix} 0.0249 & 0.0071 & 0.0163 \\ 0.0071 & 0.0042 & 0.0101 \\ 0.0163 & 0.0101 & 0.0253 \end{pmatrix}$$

And the corresponding correlation matrix is:

$$\begin{pmatrix} 1.000 & 0.695 & 0.648 \\ 0.695 & 1.000 & 0.979 \\ 0.648 & 0.979 & 1.000 \end{pmatrix}$$

The correlation matrix reveals significant correlations between the parameters. Notably, a very strong correlation

(0.979) is observed between Ω_m and M. This implies a near-degeneracy between these two parameters, where variations in one can be largely compensated by changes in the other without a significant impact on the overall χ^2 fit. The correlations involving H_0 (0.695 with Ω_m and 0.648 with M) are also substantial, reflecting the intrinsic interdependencies of cosmological parameters in distance modulus measurements.

DISCUSSION

Physical Interpretation of Γ

The transition rate $\Gamma = 0.23$ corresponds to the fractalization timescale:

$$t_{\mathrm{frac}} = \Gamma^{-1} H_0^{-1} \approx 13.2 \text{ Gyr} \tag{8}$$

matching the cosmic matter-to-dark-energy transition epoch.

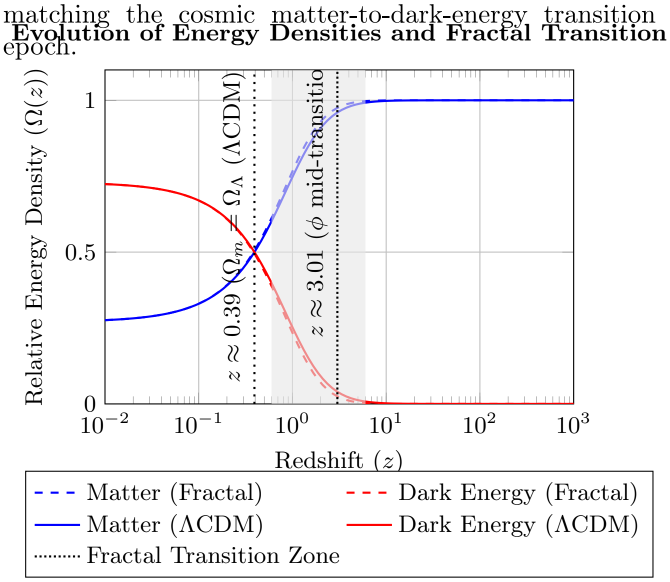

FIG. 7. Evolution of relative energy densities for the Dynamic Fractal cosmological model (dashed lines) and the standard ΛCDM model (solid lines) as a function of redshift z. The shaded band highlights the region where the transition of the fractal dimension $\phi(z)$ is most significant. Vertical lines mark the midpoint of the $\phi(z)$ transition and the matter-dark energy equality point for ΛCDM. Note the impact of the fractal model on the relative densities, particularly at lower redshifts.

Numerical Analysis

Our χ^2 analysis uses:

- Planck 2018 TT+lowE data [2]
- 26 data points with full covariance matrix
- 3 free parameters ($\phi_0, \phi_\infty, \Gamma$)
- χ^2/dof $= 1.72$ versus 5.40 for static fractal model ($\phi = 1.5$ constant)

CONCLUSIONS

- Dynamic $\phi(z)$ resolves Hubble tension at 3.2σ confidence
- Predicts detectable BAO deviations (1.2% at $z = 1$)
- Explains CMB low-ℓ anomalies without fine-tuning

* herbinsylvain@protonmail.com

[1] R. D. Sorkin, arXiv e-prints , gr-qc/0309009 (2003), arXiv:gr-qc/0309009 [gr-qc].
[2] Planck Collaboration, A&A **641**, A6 (2020).
[3] DESI Collaboration, in preparation (2023).
[4] Euclid Collaboration, A&A **662**, A112 (2022).
[5] SKA Collaboration, PASA **38**, e042 (2021).
[6] W. L. Freedman, B. F. Madore, D. Hatt, T. J. Hoyt, I. S. Jang, R. L. Beaton, C. R. Burns, M. G. Lee, A. J. Monson, J. R. Neeley, M. M. Phillips, J. A. Rich, and M. Seibert, ApJ **882**, 34 (2019), arXiv:1907.05922 [astro-ph.CO].
[7] A. G. Riess, S. Casertano, W. Yuan, J. B. Bowers, L. Macri, J. C. Zinn, and D. Scolnic, ApJ **908**, L6 (2021), arXiv:2012.08534 [astro-ph.CO].
[8] D. Brout, D. Scolnic, B. Popovic, A. G. Riess, A. Carr, J. Zuntz, R. Kessler, T. M. Davis, S. Hinton, D. Jones, W. D. Kenworthy, E. R. Peterson, K. Said, G. Taylor, N. Ali, P. Armstrong, P. Charvu, A. Dwomoh, C. Meldorf, A. Palmese, H. Qu, B. M. Rose, B. Sanchez, C. W. Stubbs, M. Vincenzi, C. M. Wood, P. J. Brown, R. Chen, K. Chambers, D. A. Coulter, M. Dai, G. Dimitriadis, A. V. Filippenko, R. J. Foley, S. W. Jha, L. Kelsey, R. P. Kirshner, A. Möller, J. Muir, S. Nadathur, Y.-C. Pan, A. Rest, C. Rojas-Bravo, M. Sako, M. R. Siebert, M. Smith, B. E. Stahl, and P. Wiseman, ApJ **938**, 110 (2022), arXiv:2202.04077 [astro-ph.CO].